Electronic Supplementary Material (ESI) for Soft Matter.

Supplementary Information

Doped photo-crosslinked polyesteramide hydrogel as solid electrolyte for supercapacitors

Jordi Tononi,[1] David Curcó,[2] Jordi Puiggalí,[1,3] Juan Torras,[1,*] and Carlos Alemán[1,3,*]

[1] *Departament d'Enginyeria Química and Barcelona Research Center for Multiscale Science and Engineering, EEBE, Universitat Politècnica de Catalunya, C/ Eduard Maristany, 10-14, 08019, Barcelona, Spain*

[2] *Departament d'Enginyeria Química i Química Analítica, Facultat de Química, Universitat de Barcelona, Martí i Franquès 1, Barcelona E-08028, Spain*

[3] *Institute for Bioengineering of Catalonia (IBEC), The Barcelona Institute of Science and Technology, Baldiri Reixac 10-12, 08028 Barcelona Spain*

Correspondence to: joan.torras@upc.edu and carlos.aleman@upc.edu

METHODS

Computational methods

All simulations were performed using the Amber18 software package.[S1] All parameters with exception of atomic charges (*i.e.* stretching, bending, torsional and van der Waals) were extrapolated from the General Amber Force Field (GAFF).[S2,S3] Atomic charges were parametrized with the RED-III program[S4,S5] using the Restrained ElectroStatic Potential (RESP) strategy[S6-S8]

Periodic boundary conditions were applied using the nearest image convention and the atom pair cut-off distance used to compute the van der Waals interactions was set at 10.0 Å. Beyond cut-off distance, electrostatic interactions were calculated by using Particle Mesh of Ewald, with a points grid density of the reciprocal space of 1 $Å^3$.[S9] The Langevin thermostat[S10] and the Berendsen barostat[S11] were used to heat the system and to rapidly equilibrate its temperature and pressure at 298 K and 1 bar, respectively. The relaxation times used for the first and second heating cycles were 15 and 5 ps, respectively, while the relaxation time for pressure was 2 ps.

All constructed systems were submitted to 20000 steps of energy minimization (Newton–Raphson method) before any MD trajectory was run in order to relax conformational and structural tensions. The temperature, density and pressure of each model were equilibrated by three consecutive MD runs. First, the systems were heated at 50 K using a NVT MD for 10 ps. After that, the temperature was increased to 298 K by running a NVT MD for another 10 ps. The resulting atom velocities and coordinates were used as the starting point for a NPT-MD run (298 K, 1 bar pressure) that was enlarged until the variation of the density was lower than 1%. The end of this simulation was the starting point of the productive trajectories presented in this work (298 K, 1 bar pressure), which took 200 ns for each simulated system.

Synthesis of UPEA-Phe hydrogels

The synthesis of UPEA-Phe and its subsequent reticulation with functionalized PEG was exhaustively described in previous work.[S12,S13]

Chemical and morphological characterization of hydrogels

Infrared absorption spectra were recorded with a Fourier Transform FTIR 4100 Jasco spectrometer in the 4000–600 cm^{-1} range. A Specac Model MKII Golden Gate attenuated total reflection (ATR) cell with a heated Diamond ATR Top-Plate was used.

The morphology of the photo-crosslinked UPEA-Phe hydrogels was observed by scanning electron microscopy (SEM) using a Focused Ion Beam Zeiss Neon40 scanning electron microscope equipped with an energy dispersive X-ray (EDX) spectroscopy system and operating at 5 kV. All samples were sputter-coated with a thin carbon layer using a K950X Turbo Evaporator to prevent electron charging problems. Prior to SEM observation, samples were lyophilized. Thus, throughout the freeze-drying process, the capillary stress is avoided, preventing the collapse of the structure and minimizing the shrinkage of the material. The size of pores was determined from the SEM images using the software SmartTIFF (v1.0.1.2.).

Synthesis and characterization of electrodes

Poly(3,4-ethylenedioxythiophene) electrodes were prepared by methods already described.[S14] Briefly, PEDOT was obtained by anodic polymerization in acetonitrile at a constant potential of 1.25 V imposing a polymerization charge equal to 500 mC/cm^2 (at room temperature and nitrogen atmosphere). The mass of PEDOT deposited onto the WE (m_{pol}= 1.127 ± 0.203 mg) was determined as the weight difference between coated

and uncoated steel sheets (n = 20) using a CPA26P Sartorius analytical microbalance with a precision of 10^{-6} g. The electrical conductivity, average thickness and root-mean-square roughness of PEDOT films was 29 ± 1 S/cm, 4.1 ± 0.6 μm and 0.5 ± 0.1 μm, respectively.

Electrochemical characterization

The response of electrochemical supercapacitors (ESCs), which were prepared as is described in the main text using PEDOT electrodes and hydrogel solid electrolytes, was studied in a two-electrode configuration by means of cyclic voltammetry (CV) and galvanostatic charge-discharge (GCD) measurements.

The specific capacitance (*SC*; in F/g) is the capacitance per unit of mass for one electrode, is expressed as:

$$SC = 4 \times \frac{C}{m} \tag{S1}$$

where C is the measured capacitance for the two-electrode cell and m the total mass of the active material in both electrodes. The multiplier 4 adjusts the capacitance of the cell and the combined mass of the two electrodes to the capacitance and mass of a single electrode.

CV measurements were used to provide information regarding the cell capacitance (C, F) by applying Eq S2:

$$C = I \Big/ \left(\frac{dV}{dt}\right) \tag{S2}$$

where I corresponds to the average current during discharging and dV/dt is the scan rate. For the ESC devices studied in this work, CV curves were recorded from 0.0 V to 0.8 V at several scan rates: 10, 25, 50, 75, 100, 150 and 200 mV/s.

The cell capacitance was also determined using the GCD procedure and applying Eqn S2. In this case, *I* is the discharging current applied to the device and *dV/dt* should be calculated as $(V_{max} - ½V_{max})/(t_2 - t_1)$, where V_{max} corresponds to the highest voltage in the GCD curve after the voltage drop (V_{drop}) at the beginning of the discharging process. GCD curves were run at different current densities (*i.e.* charge and discharge rates are specified in units of current per electrode mass): 0.43, 0.61, 1.22 and 2.44 A/g, which corresponded to 0.5, 0.7, 1.4 and 2.8 mA, respectively.

The Coulombic efficiency (η, %) was evaluated as the ratio between the discharging and charging times (t_d and t_c, respectively) for the electrochemical window between 0.0 V and 0.8 V:

$$\eta = {}^{t_d}\!/_{t_c} \qquad (3)$$

On the other hand, the cycling stability of the selected ESCs was tested by submitting the system to: *(i)* 1400 GCD cycles at a current density of 1.22 A/g from 0.0 V to 0.8 V, which corresponds to t_c and t_d of approximately 40-60 seconds; and *(ii)* 200 CV cycles at a scan rate of 50 mV/s from 0.0 V (initial and final potential) to 0.8 V (reversal potential). Moreover, the self-discharging and the leakage current (LC) curves were evaluated by applying the following methodologies. In the first case, ESC devices were charged to 0.8 V at 0.25 mA and kept at $1 \cdot 10^{-11}$ mA for 10 min (*i.e.* self-discharging). After that time, the device was discharged to 0 V at –1 mA. In the second case, after charging the devices to 0.8 V at 0.25 mA, they were kept at 0.8 V for 300-600 s while recording the current data through the ESC (*i.e.* leakage current). Data were obtained from testing three independent samples for each device.

SUPPLEMENTARY REFERENCES

S1. D. A. Case, I. Y. Ben-Shalom, S. R. Brozell, D. S. Cerutti, T. E. Cheatham III, V. W. D. Cruzeiro, T. A. Darden, R. E. Duke, D. Ghoreishi, M. K. Gilson, H. Gohlke, A. W. Goetz, D. Greene, R. Harris, N. Homeyer, S. Izadi, A. Kovalenko, T. Kurtzman, T. S. Lee, S. LeGrand, P. Li, C. Lin, J. Liu, T. Luchko, R. Luo, D. J. Mermelstein, K. M. Merz, Y. Miao, G. Monard, C. Nguyen, H. Nguyen, I. Omelyan, A. Onufriev, F. Pan, R. Qi, D. R. Roe, A. Roitberg, C. Sagui, S. Schott-Verdugo, J. Shen, C. L. Simmerling, J. Smith, R. Salomon-Ferrer, J. Swails, R. C. Walker, J. Wang, H. Wei, R. M. Wolf, X. Wu, L. Xiao, D. M. York and P. A. Kollman, AMBER 2018, University of California, San Francisco, 2018.

S2 J. Wang, W. Wang, P. A. Kollman and D. A. Case, *J. Mol. Graph. Model.*, 2006, **25**, 247–260.

S3 J. Wang, R. M. Wolf, J. W. Caldwell, P. A. Kollman and D. A. Case, *J. Comput. Chem.*, 2004, **25**, 1157–1174.

S4. F.-Y. Dupradeau, A. Pigache, T. Zaffran, C. Savineau, R. Lelong, N. Grivel, D. Lelong, W. Rosanski and P. Cieplak, *Phys. Chem. Chem. Phys.*, 2010, **12**, 7821−7839,

S5. A. Pigache, P. Cieplak and F.-Y. Dupradeau, Automatic and highly reproducible RESP and ESP charge derivation: Application to the development of programs RED and XRED, *227th ACS National Meeting*, Anaheim, CA, USA, March 28 - April 1, **2004**

S6. C. I. Bayly, P. Cieplak, W. D. Cornell and P. A. Kollman, *J. Phys. Chem.*, 1993, **97**, 10269−10280.

S7. W. D. Cornell, P. Cieplak, C. I. Bayly and P. A. Kollman, *J. Am. Chem. Soc.*, 1993, **115**, 9620−9631.

S8. P. Cieplak, W. D. Cornell, C. Bayly and P. A. Kollman, *J. Comput. Chem.*, 1995, **16**, 1357−1377.

S9. T. Darden, D. York and L. Pedersen, *J. Chem*. *Phys*., 1993, **98**, 10089−10092.

S10. R. L. Davidchack, R. Handel and M. V. Tretyakov, *J. Chem. Phys.*, 2009, **130**, 234101.

S11. H. J. C. Berendsen, J. P. M. Postma, W. F. van Gunsteren, A. DiNola and J. R. Haak, *J. Chem. Phys.*, 1984, **81**, 3684-3690.

S12. G. Ruano, A. Díaz, J. Tononi, J. Torras, J. Puiggalí and C. Alemán, *Polym. Test.*, 2020, **82**, 106300.

S13. K. Guo, C. C. Chu, E. Chkhaidze and R. Katsarava, *J. Polym. Sci.; Part A: Polym. Chem.*, 2005, **43**, 1463–1477.

S14. E. Armelin, M. M. Pérez-Madrigal, C. Alemán and D. D. Díaz, *J. Mater. Chem. A*, 2016, **4**, 8952−8968. *J. Mater. Chem. A* **2016**, *4*, 1792–1805.

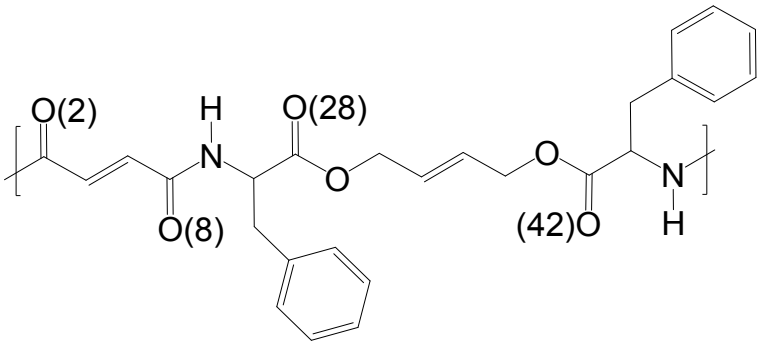

Scheme S1. Structure of the UPE-Phe displaying the labels used to identify the oxygen atoms for the analyses of MD trajectories.

Table S1. Number of explicit water molecules considered for simulations of the UPEA-Phe hydrogel as a function of the cross-linking degree and the hydration. The number of NaCl molecules added to reach a 0.1 M NaCl concentration is displayed in parenthesis.

Cross-linking degree	**Number of explicit water**		
	100% w/w	**300% w/w**	**500% w/w**
17%	6724 (12)	18155 (33)	30645 (55)
25%	8972 (16)	27584 (50)	45737 (82)
35%	16444 (29)	48136 (86)	80478 (144)

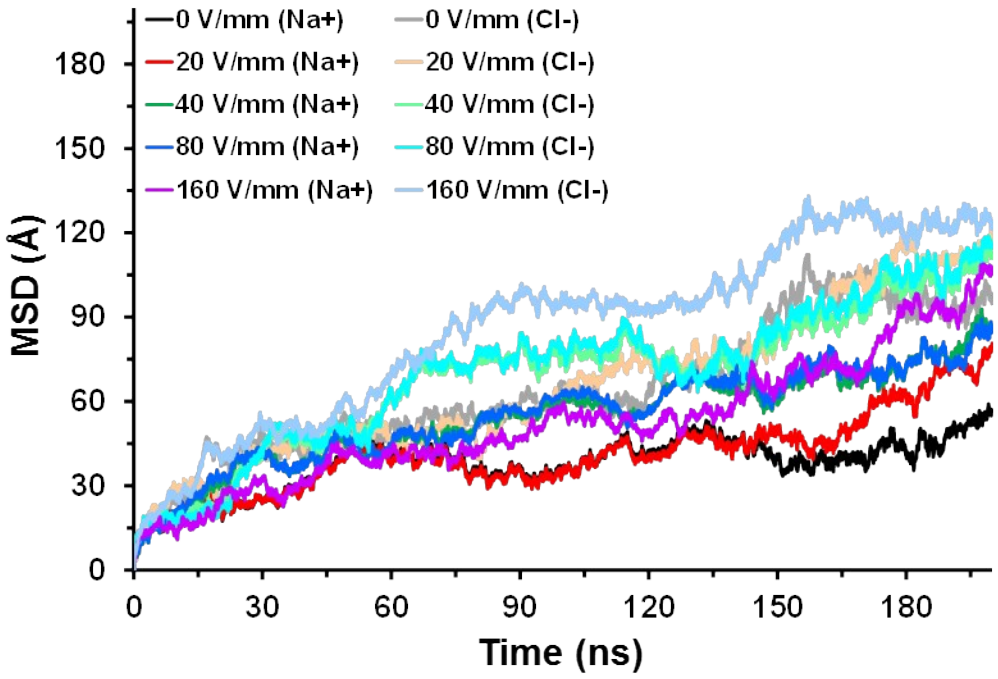

Figure S1. MSD for the system for UPEA-Phe/NaCl with CLD= 17% and HD= 100%.

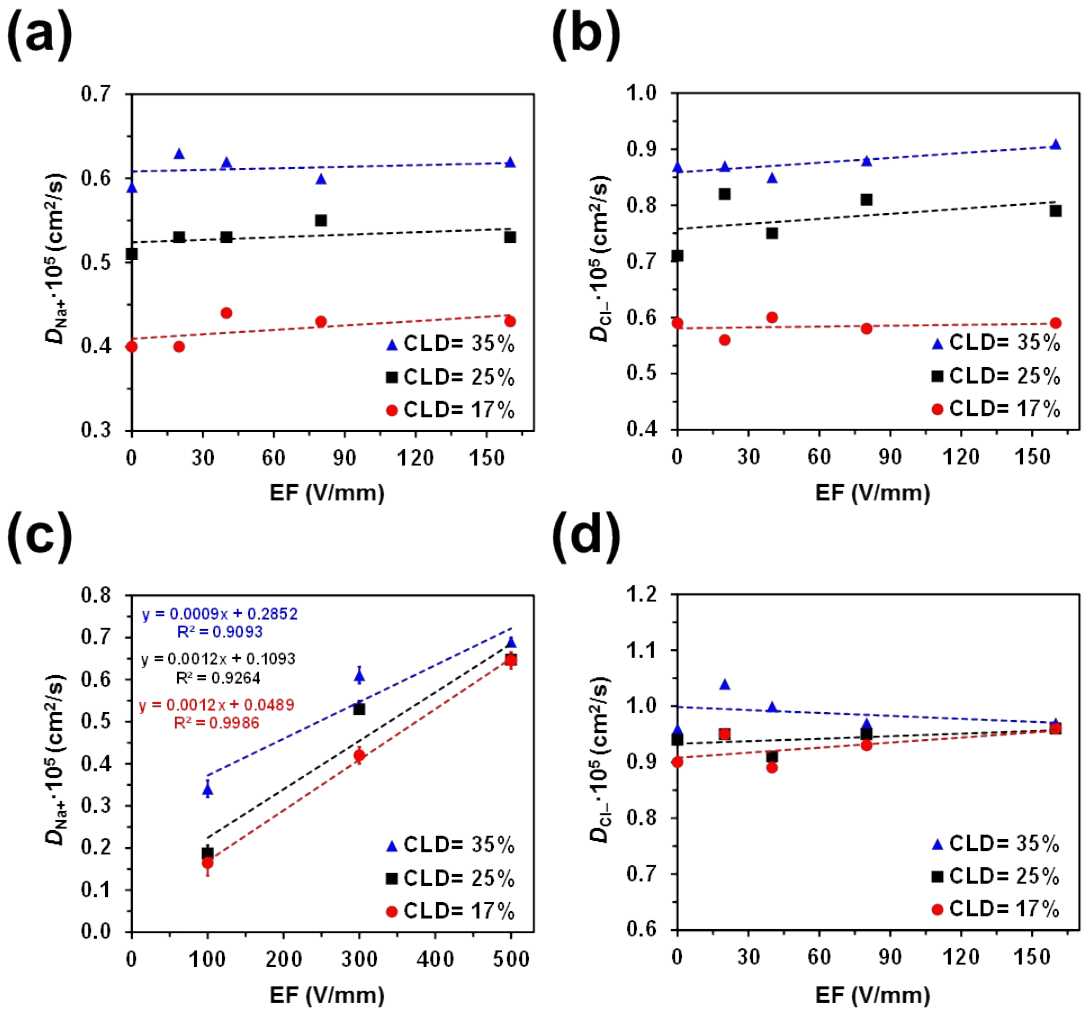

Figure S2. Variation of the diffusion coefficients of (a, c) Na^+ and (b, d) Cl^- (D_{Na+} and D_{Cl-}, respectively) against the strength of the electric field (EF) for UPA-Phe/NaCl hydrogels with (a, b) HD= 300% and (c, d) HD= 500% (*i.e.* profiles for hydrogels with HD= 100% are shown in Figures 2a and 2b).

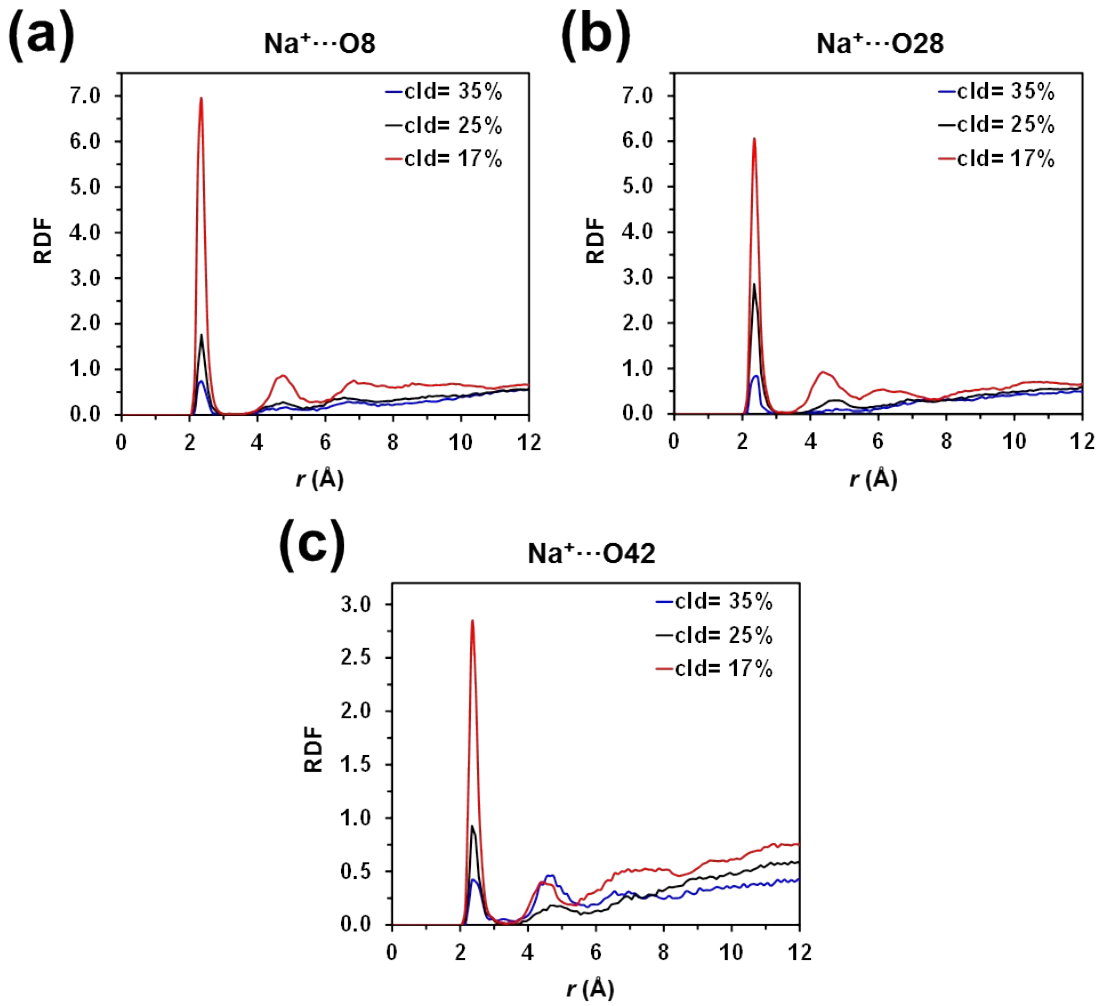

Figure S3. Radial distribution functions (RDF) for (a) $Na^{+}\cdots O8$, (b) $Na^{+}\cdots O28$ and (c) $Na^{+}\cdots O42$ atom pairs. Data correspond to simulations of hydrogels with different cld and hd= 100%.

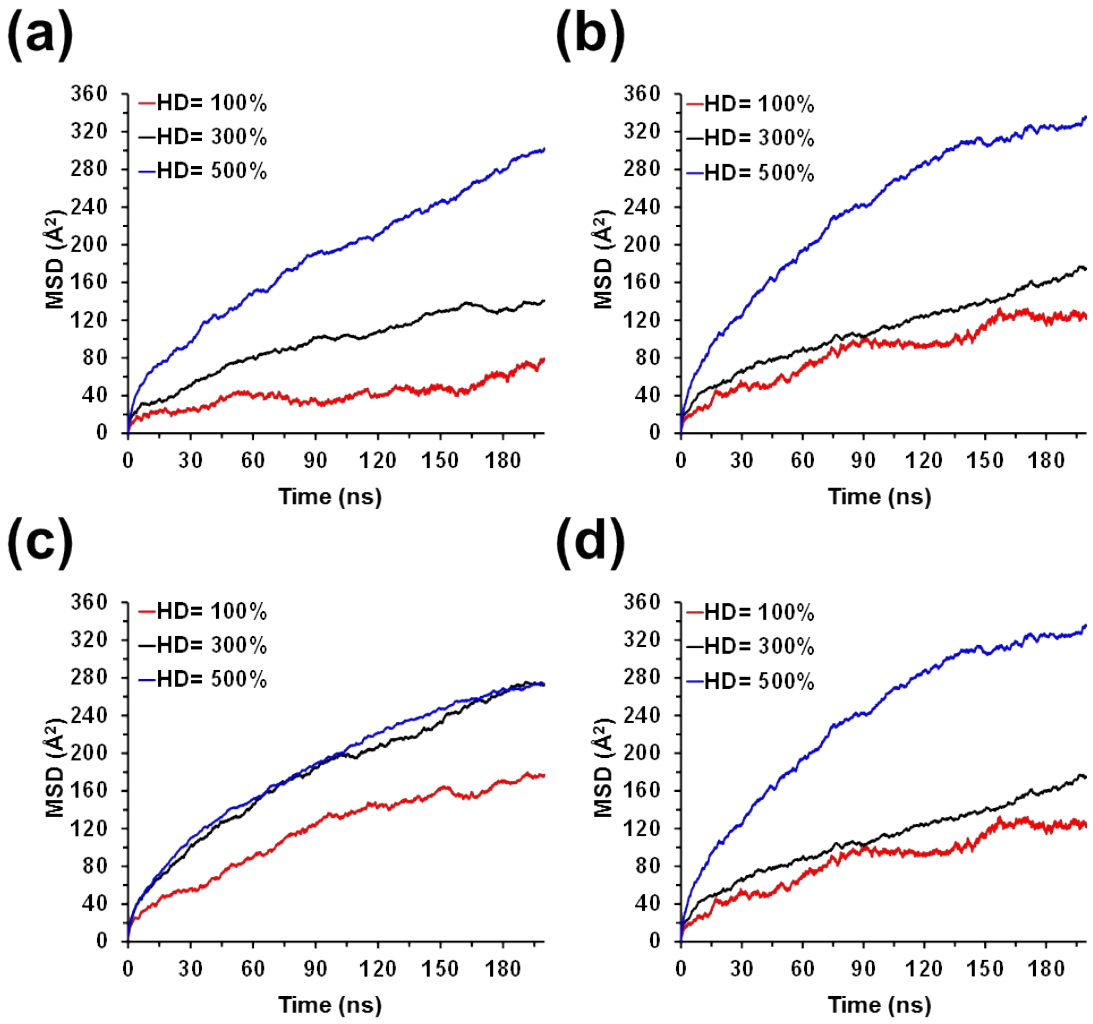

Figure S4. The temporal evolution of the MSD for (a, c) Na^+ and (b, d) Cl^- ions in doped hydrogels with (a, b) CLD= 17% and (c, d) CLD= 35% using EF= 20 V/mm (results for the system with CLD= 25% are shown in Figure 2e-f)